International Journal of Electrical, Electronic and Communication Sciences
ISSN: 2517-9438
Vol:2, No:10, 2008

Investigating the Impact of Wind Speed on Active and Reactive Power Penetration to the Distribution Network

Sidhartha Panda, N.P.Padhy

***Abstract*—**Wind power is among the most actively developing distributed generation (DG) technology. Majority of the wind power based DG technologies employ wind turbine induction generators (WTIG) instead of synchronous generators, for the technical advantages like: reduced size, increased robustness, lower cost, and increased electromechanical damping. However, dynamic changes of wind speed make the amount of active/reactive power injected/drawn to a WTIG embedded distribution network highly variable. This paper analyzes the effect of wind speed changes on the active and reactive power penetration to the wind energy embedded distribution network. Four types of wind speed changes namely; constant, linear change, gust change and random change of wind speed are considered in the analysis. The study is carried out by three-phase, non-linear, dynamic simulation of distribution system component models. Results obtained from the investigation are presented and discussed.

***Keywords*—**Wind turbine induction generator, distribution network, active and reactive power, wind speed.

NOMENCLATURE

Wind Turbine:

P_m	Mechanical output power of the turbine (W).
C_P	Performance coefficient of the turbine.
ρ	Air density (kg/m^3).
A	Turbine swept area (m^2).
V_{wind}	Wind speed (m/s).
λ	Tip speed ratio of the rotor blade tip speed to wind speed.
β	Blade pitch angle (deg).
P_{m_pu}	Power in pu of nominal power for particular values of ρ and A.
k_p	Power gain.
C_{P_pu}	Performance coefficient in pu of the maximum value of C_P.

Induction Machine:

R_s, L_{ls}	Stator resistance and leakage inductance.
R'_r, L'_{lr}	Rotor resistance and leakage inductance.
L_m	Magnetizing inductance.
L_s, L'_r	Total stator and rotor inductances.
V_{qs}, i_{qs}	q-axis stator voltage and current.
V'_{qr}, i'_{qr}	q-axis rotor voltage and current.
V_{ds}, i_{ds}	d-axis stator voltage and current.
V'_{dr}, i'_{dr}	d-axis rotor voltage and current.
φ_{qs}, φ_{ds}	Stator q and d-axis fluxes.
φ'_{qr}, φ'_{dr}	Rotor q and d-axis fluxes.
ω_m	Angular velocity of the rotor.
θ_m	Rotor angular position.
P	Number of pole pairs.
ω_r	Electrical angular velocity.
θ_r	Electrical rotor angular position.
T_e	Electromagnetic torque.
J	Combined rotor and load inertia coefficient.
H	Combined rotor and load inertia constant.
F	Combined rotor and load viscous friction coefficient.

Sidhartha Panda is a research scholar in the Department of Electrical Engineering, Indian Institute of Technology, Roorkee, Uttaranchal, 247667, India. (e-mail: panda_sidhartha@rediffmail.com).

N.P.Padhy is Associate professor in the Department of Electrical Engineering, IIT, Roorkee India.(e-mail:, nppeefee@iitr.ernet.in)

I. INTRODUCTION

THE rapid development of distributed generation (DG) technology is gradually reshaping the conventional power systems in a number of countries. Wind power is among the most actively developing distributed generation. Grid-connected wind capacity is undergoing the fastest rate of growth of any form of electricity generation, achieving global annual growth rates on the order of 20 - 30% [1]. The

presence of wind power generation is likely to influence the operation of the existing power system networks [2]-[3]. Dynamic changes of wind speed make amount of power injected to a network highly variable. Depending on intensity and rate of changes, difficulties with frequency, voltage regulation and stability, could make a direct impact to quality level of delivered electrical energy [4]. In this context, connection of wind turbine generator with dispersed generation of electricity, calls for a detailed technical analysis.

Majority of the wind power based DG technologies employ induction generators instead of synchronous generators, for the technical advantages of induction machines like: reduced size, increased robustness, lower cost, and increased electromechanical damping [5]. Wind turbine induction generator (WTIG) can be viewed as a consumer of reactive power. Its reactive power consumption depends on active power production. With the variation in the wind speed, the active power generation and hence the reactive power drawn/supplied by the WTIGs from the distribution network varies.

In this work the effect of wind speed changes on the penetration of active and reactive power to the distribution network is investigated. Various types of wind speed changes namely, constant wind speed, linear change of wind speed, gust change of wind speed and random change of wind speed are considered in the present study. The study is based on the three phase non-linear dynamic simulation, utilizing the SimPowerSystem blockset for use with MATLAB/SIMULINK [6]. Simulation results are presented to show dynamic performance of a distributed network embedded with WTIGs under various types of changes in wind speed.

II. Wind Turbine Induction Generator (WTIG)

The block diagram of wind turbine the induction generator (WTIG) is shown in Fig. 1. The stator winding is connected directly to the 60 HZ grid and the rotor is driven by a variable-pitch wind turbine. The power captured by the wind turbine is converted into electrical power by the induction generator and is transmitted to the grid by the stator winding. The pitch angle is controlled in order to limit the generator output power to its nominal value for high wind speeds. In order to generate power the induction generator speed must be slightly above the synchronous speed.

The pitch angle controller regulates the wind turbine blade pitch angle β, according to the wind speed variations. Hence, the power output of WTIG depends on the characteristics of the pitch controller in addition to the turbine and generator characteristics. This control guarantees that, irrespective of the voltage, the power output of the WTIG for any wind speed will be equal to the designed value for that speed. This designed power output of the WTIG with wind speed is provided by the manufacturer in the form of a power curve. Hence, for a given wind speed, power output can be obtained from the power curve of the WTIG.

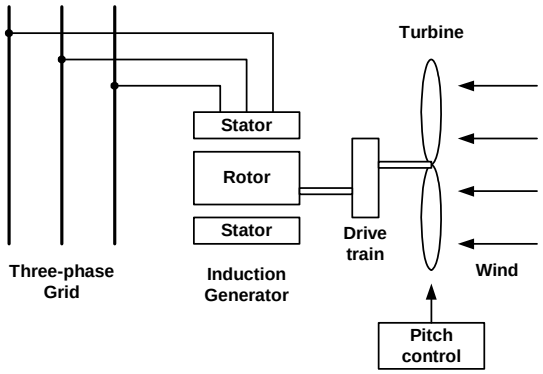

Fig. 1 Block diagram of wind turbine induction generator

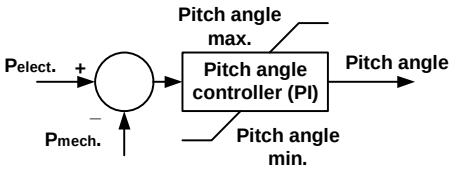

Fig. 2 Control system for pitch angle control

The pitch angle β is controlled in order to limit the generator output power at its nominal value for winds exceeding the nominal speed. β is controlled by a Proportional-Integral (PI) controller in order to limit the electric output power to the nominal mechanical power. When the measured electric output power is under its nominal value, β is kept constant at zero degree. When it increases above its nominal value the PI controller increases β to bring back the measured power to its nominal value. The pitch angle control system is shown in Fig. 2. In order to generate power the IG speed must be slightly above the synchronous speed. Speed varies approximately between 1 pu at no load and 1.005 pu at full load.

A. Wind Turbine

The wind turbine model is employed in the present study is based on the steady-state power characteristics of the turbine. The stiffness of the drive train is infinite and the friction factor and the inertia of the turbine are combined with those of the generator coupled to the turbine. The wind turbine mechanical power output is a function of rotor speed as well as the wind speed and is expressed as:

$$P_m = C_P(\lambda,\beta)\frac{\rho A}{2}V^3_{wind} \quad (1)$$

Normalizing (1) in the per unit (pu) system as:

$$P_{m\_pu} = k_p C_{P\_pu}\ V^3_{wind\_pu} \quad (2)$$

A generic equation is used to model $C_P(\lambda, \beta)$. This equation, based on the modeling turbine characteristics is [11]:

$$C_P(\lambda,\beta) = c_1\left(\frac{c_2}{\lambda_i} - c_3\beta - c_4\right)e^{\frac{-c_5}{\lambda_i}} + c_6\lambda \quad (3)$$

With

$$\frac{1}{\lambda_i} = \frac{1}{\lambda + 0.08\beta} - \frac{0.035}{\beta^3 + 1} \quad (4)$$

The relevant parameters are given in appendix.

B. Induction Machine

In the present study, the electrical part of the machine is represented by a second-order state-space model and the mechanical part by a second-order system. All electrical variables and parameters are referred to the stator. All stator and rotor quantities are in the arbitrary two-axis reference frame (d-q frame). The d-axis and q-axis block diagram of the electrical system is shown in Figs. 3 (a) and 3 (b).

The electrical equations are given by:

$$v_{qs} = R_s i_{qs} + \frac{d}{dt}\varphi_{qs} + \omega\varphi_{ds} \quad (5)$$

$$v_{ds} = R_s i_{ds} + \frac{d}{dt}\varphi_{ds} - \omega\varphi_{qs} \quad (6)$$

$$v'_{qr} = R'_r\, i_{qr} + \frac{d}{dt}\varphi'_{qr} + (\omega - \omega_r)\varphi'_{dr} \quad (7)$$

$$v'_{dr} = R'_r\, i_{dr} + \frac{d}{dt}\varphi'_{dr} - (\omega - \omega_r)\varphi'_{qr} \quad (8)$$

$$T_e = 1.5\,p(\varphi_{ds} i_{qs} - \varphi_{qs} i_{ds}) \quad (9)$$

where,

$$\varphi_{qs} = L_s i_{qs} + L_m i'_{qr}$$

$$\varphi_{ds} = L_s i_{ds} + L_m i'_{dr}$$

$$\varphi'_{qr} = L'_r\, i'_{qr} + L_m i_{qs}$$

$$\varphi'_{dr} = L'_r\, i'_{dr} + L_m i_{ds}$$

with $L_s = L_{ls} + L_m$ and $L'_r = L'_{lr} + L_m$

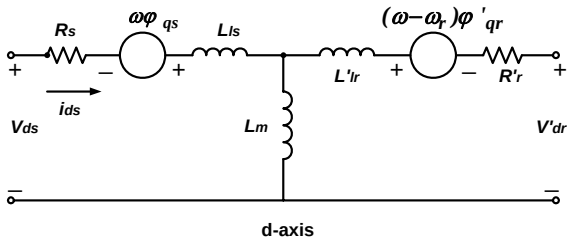

(a)

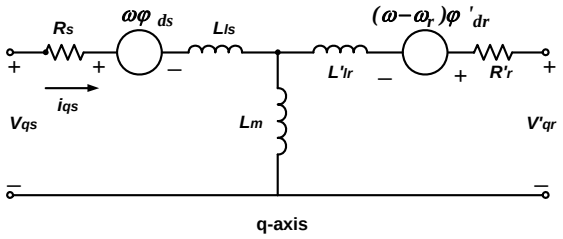

(b)

Fig. 3 Induction machine equivalent circuits (a) *d*-axis equivalent circuit (b) *q*-axis equivalent circuit

The mechanical equations are given by:

$$\frac{d}{dt}\omega_m = \frac{1}{2H}(T_e - F\omega_m - T_m) \quad (10)$$

$$\frac{d}{dt}\theta_m = \omega_m \quad (11)$$

III. System Under Study

Distribution systems are inherently unbalanced in most of the cases due to the asymmetrical line spacing and imbalance of customer load. In view of this, single phase models can not be used for accurate studies on the operation of distributed systems. Therefore in this work all network components are represented by the three-phase models. Wind turbines use squirrel-cage induction generators. The stator winding is connected directly to the 60 Hz grid and the rotor is driven by a variable-pitch wind turbine. In order to limit the generator output power at its nominal value, the pitch angle is controlled for winds exceeding the nominal speed of 9 m/s. To inject active power to the distribution network, the WTIG speed must be slightly above the synchronous speed. Speed varies approximately between 1 pu at no load and 1.005 pu at full load.

The one line diagram of the test system employed in this study is shown in Fig. 4. The network consists of a 132 kV, 60-Hz, sub-transmission system with short circuit level of 2500 MVA, feeds a 33 kV distribution system through 132/33 kV step down transformers. Three WTIGs of rating 1.5 MW, 3 MW and 4.5 MW connected to bus 3, bus 4 and bus 5 respectively, export power to the 132 kV grid through radial feeders. Reactive power compensation is provided to compensate for the large reactive currents drawn by WTIGs. The reactive powers consumed by the WTIGs are locally supplied by fixed capacitors of 250 kVAR, 500 kVAR and 1000 kVAR for 1.5 MW, 3 MW and 4.5 MW WTIGs respectively, each being installed at the terminals of the machines as shown in Fig. 4. All the relevant data are given in appendix.

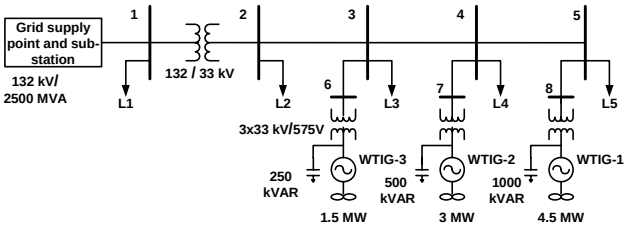

Fig. 4 Single-line diagram of the distribution system embedded with wind turbine induction generators

IV. Simulation Results

The dynamic behavior of the WTIGs and the amount of active/reactive power drawn/injected from/to grid during wind speed changes is analyzed and presented in this section. Four types of wind speed namely; constant wind speed, linear change of wind speed, gust change of wind speed and random change of wind speed as shown in Fig. 5 are considered in the present study. In the Figs. P_{G1}, P_{G2} and P_{G3} represent the active power generation of WTIG-1 (4.5 MW), WTIG-2 (3 MW) and WTIG-3 (1.5 MW) respectively. The reactive power generations are represented by Q_{G1}, Q_{G2} and Q_{G3} for WTIG-1, WTIG-2 and WTIG-3 respectively.

A. Constant Wind Speed

A constant wind speed of 8 m/s is applied to WTIGs. The active and reactive power generations of WTIGs is shown in Fig. 6. It can be seen from Fig. 6 that, WTIG-1 whose rated

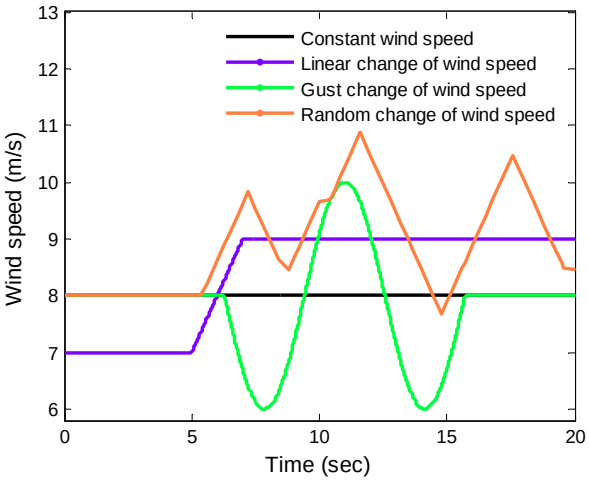

Fig. 5 Types of wind speed

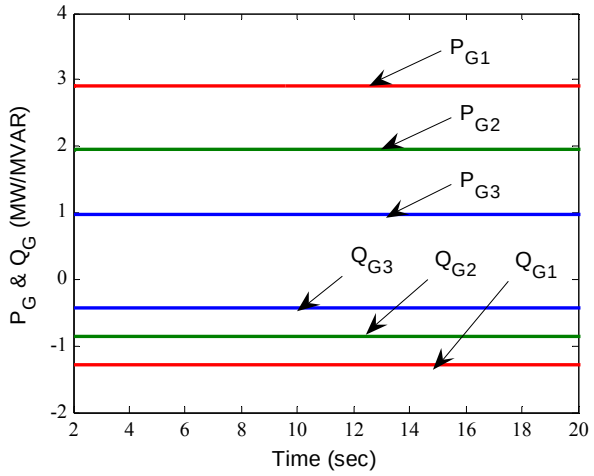

Fig. 6 Active and reactive power generation by WTIGs at constant wind speed

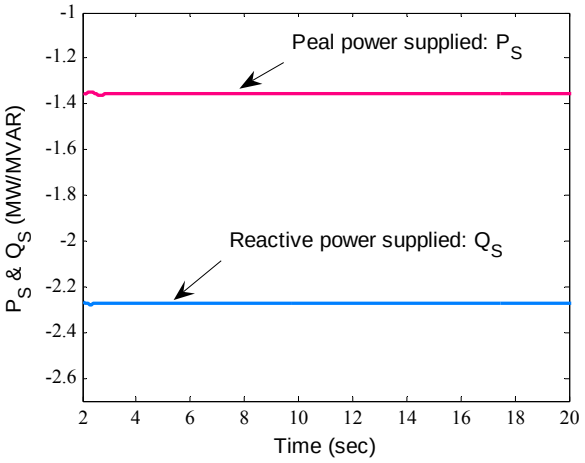

Fig. 7 Active and reactive power supplied by WTIGs to the grid for constant wind speed

output is 4.5 MW at a wind speed of 9 m/s, generates 2.905 MW at constant wind speed of 8 m/s. The negative reactive power generation Q_{G1} indicates that WTIG-1 consumes 1.29 MVAR of reactive power at constant wind speed of 8 m/s. The corresponding values for WTIG-2 and WTIG-3 are 1.943 MW and 0.975 MW of real power generation; and 0.895 MVAR and 0.4293 MVAR of reactive power consumption respectively.

As the total active power generation by the WTIGs at constant wind speed of 8 m/s is less than the total load present in the distribution system, the difference active power is drawn from the grid. The active and reactive power supplied by WTIGs to the grid for constant wind speed of 8 m/s is shown in Fig. 7, where the negative values indicate that powers are drawn from grid. It can be seen from Fig. 7 that, in this case, 1.3556 MW of active power and 2.2773 MVAR of reactive power is drawn from the grid.

B. *Linear Change of Wind Speed*

A linear change of wind speed as shown in Fig. 5 is applied to the WTIGs. This type of wind speed change enables the WTIGs to inject active power into a network from minimum to maximum value in a manner slow enough not to induce unwanted oscillations.

Fig. 8 shows the real and reactive power generations of WTIGs for a linear change of wind speed from 7 m/s to 9 m/s. it can be seen from Fig. 8 that, at lower wind speed of 7 m/s, the real power generation and reactive power consumption of WTIG-1 are 1.559 MW and 0.8989 MVAR respectively. But as the wind speed increases to 9 m/s, the real power generation of WTIG-1 increases to 4.325 MW and hence the reactive power consumption also increases to 2.128 MVAR. The corresponding values for WTIG-2 and WTIG-3 are 1.014 MW and 0.5217 MW of real power generation respectively at lower wind speed (7 m/s) with reactive power consumption of 0.5948 MVAR and 0.2963 MVAR respectively. At higher wind speed of 9 m/s, the real power generation of WTIG-2 and WTIG-3 increase to 2.901 MW and 1.459 MW respectively with 1.417 MVAR and 0.7049 MVAR of reactive power consumption respectively.

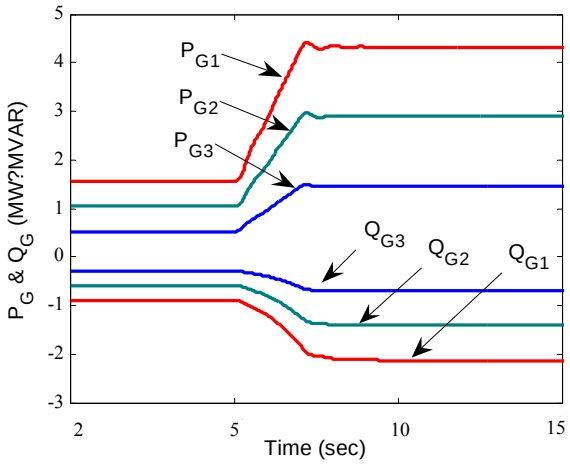

Fig. 8 Active and reactive power generation by WTIGs for linear change of wind speed

At lower wind speed of 7 m/s, the total active power generation by the WTIGs is less than the total load present in the distribution system and hence the difference active power is drawn from the grid. But at higher wind speed of 9 m/s, the WTIGs active power generation exceeds the total load present in the distribution system and hence the difference power is supplied to the grid. The active and reactive power supplied by WTIGs to the grid for linear change of wind speed from 7 m/s to 9 m/s is shown in Fig. 9, where the negative values indicate that powers are drawn from grid. It can be seen from Fig. 9 that, at lower wind speed of 7 m/s, 4.019 MW of active power and 1.05 MVAR of reactive power are drawn from the grid. But as the wind speed changes to 9 m/s, active power generated by WTIGs exceeds the total load in the distribution system and hence the excess active power is injected to the grid. It can be seen from Fig. 9 that, at a wind speed of 9 m/s, 1.429 MW of active power is injected to the distribution grid. With increase in active power generation, the reactive power consumption of WTIGs increases and so 5.101 MVAR of reactive power are drawn from the grid.

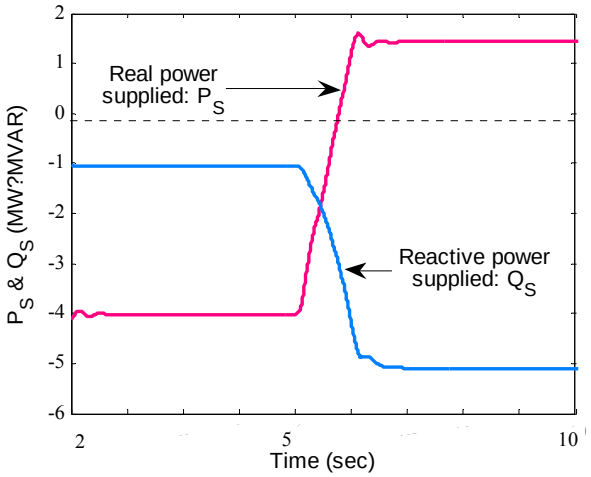

Fig. 9 Active and reactive power supplied by WTIGs to the grid for linear change of wind speed

C. *Gust Change of Wind Speed*

Gust change of the wind speed is applied here investigate its effect on power exchange between the WTIGs and the distribution network. The gust change is defined as periods of 9.47 s with 25 % maximum deviation from the initial value of the wind speed equal to 8 m/s as shown in Fig. 5. With gust change in wind speed, the active power generation of WTIGs varies in the same manner (i.e. decreases with decrease in wind speed and vice versa). The reactive power consumption of WTIGs being proportional to the active power generation also varies in the same manner. The active and reactive power generation of WTIGs for gust change in wind speed is shown in Fig. 10.

It can been from Fig. 10 that, at the minimum wind speed of 6 m/s, the active power generation of WTIG-1 drops to 0.3962 MW with a reactive power consumption of 0.7407 MVAR. At the maximum wind speed of 10 m/s the active power generation of WTIG-1 is 5.042 MW and reactive power consumption is 2.547 MVAR. The minimum and maximum generations of WTIG-2 are 0.2705 MW and 3.374 MW active powers respectively. The reactive power consumptions are 0.4914 MVAR and 1.692 MVAR at minimum and maximum active power generations. For WTIG-3, the minimum and maximum generations are 0.1378 MW and 1.459 MW of active powers respectively. The reactive power consumptions are 0.2462 MVAR and 0.7049 MVAR at minimum and maximum active power generations.

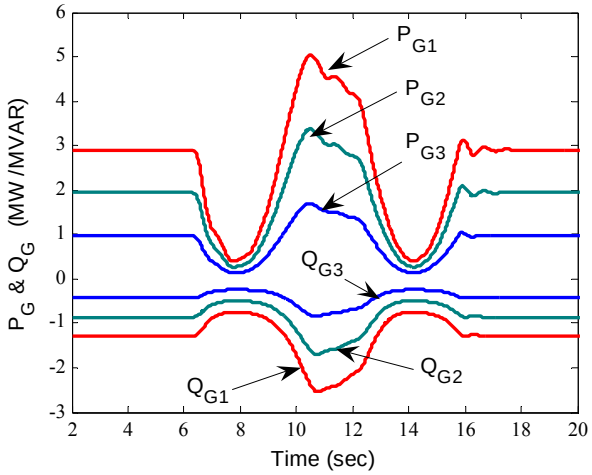

Fig. 10 Active and reactive power generation by WTIGs for gust change of wind speed

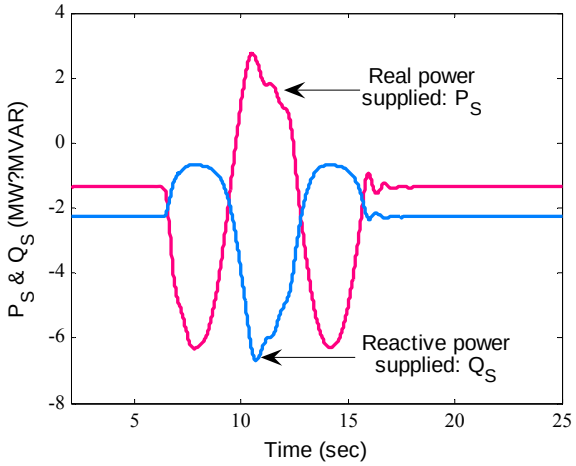

Fig. 11 Active and reactive power supplied by WTIGs to the grid for gust change of wind speed

The active and reactive power supplied by WTIGs to the distribution grid for gust change of wind speed is shown in Fig. 11. It can be seen from Fig. 11 that, active power is exchanged in both the directions (from and to the grid) and reactive power drawn from the grid also varies drastically. At minimum wind speed of 6 m/s, 6.319 MW of active power and 0.6752 MVAR of reactive power are drawn from the grid. But at the maximum wind speed of 10 m/s, active power generated by WTIGs exceeds the total load in the distribution system and hence the excess active power is injected to the grid. It can be seen from Fig. 11 that, at maximum wind speed of 10 m/s, 2.765 MW of active power is injected to the distribution grid and 6.703 MVAR of reactive power are drawn from the grid.

D. Random Change of Wind Speed

In order to investigate the effect of random change of wind speed on power exchange between the WTIGs and the distribution network, random change of wind speed shown in Fig. 5 is considered. The active and reactive power generations are shown in Fig. 12. It is clear from the Fig. 12 that, both active and reactive power generation of WTIGs vary in the same random manner.

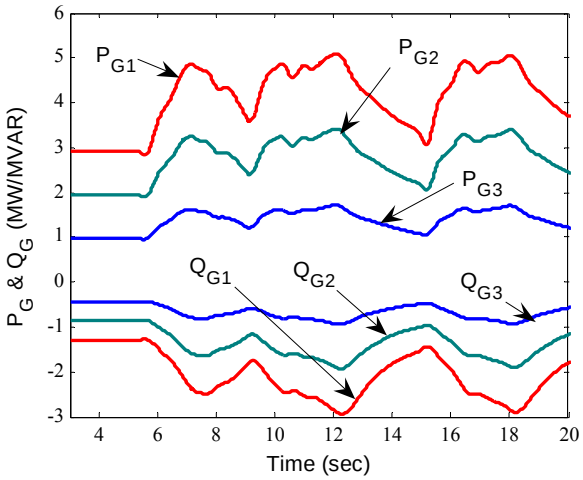

Fig. 12 Active and reactive power generation by WTIGs for random change of wind speed

At the maximum wind speed of 11 m/s the active power generation of WTIG-1 is 5.091 MW and reactive power consumption is 2.946 MVAR. The active power generation drops to 3.061 MW at the minimum wind speed of 7.67 m/s, with the reactive power consumption of 1.432 MVAR. The maximum and minimum generations of WTIG-2 are 3.423 MW and 2.071 MW active powers respectively. The reactive power consumptions are 1.931 MVAR and 0.9524 MVAR at maximum and minimum active power generations. For WTIG-3, the maximum and minimum generations are 1.725 MW and 1.053 MW of active powers respectively. The reactive power consumptions are 0.9368 MVAR and 0.4773 MVAR at maximum and minimum active power generations.

V. Conclusion

This paper investigates the effect of wind speed changes on the active and reactive power penetration to the wind energy embedded distribution network. The active power generated by the WTIGs depends upon the wind speed. With the variation in active power generation, the reactive power consumption also varies. When the reactive power requirements of WTIGs exceed the reactive power supplied by the fixed capacitors, the difference reactive power is drawn from the grid. At lower active power generation, reactive power is supplied to the grid due to the less consumption of reactive powers by the WTIGs. But at higher active power generations, active power is injected to the grid and reactive power is drawn form the grid.

Appendix

Example distribution system data (All data are in pu unless specified otherwise; the notations used are defined in [6]).

Transformer parameters:

Substation: 47 MVA, 1320/33 kV, R_2=0.0026, L_2=0.08, R_m=500Ω, X_m=500 Ω.

WTIG to distribution network: 33 kV/575 V, R_2=0.0008, L_2=0.025, R_m=500Ω, X_m= inf.

Transmission line parameters per km:

R_1=0.1153 Ω, R_0=0.413 Ω, L_1=1.05 mH, L_0=3.32 mH, C_1=11.33 nF, C_0=5.01nF.

Line lengths:

bus 2-3 & 3-4:25 km, bus 4-5:10 km, bus 3-6, 4-7 &5-8:1 km.

Loads (kW + j kVAR):

Load 1:5000+j1000; Loads 2,3, 4 & 5:500+j20.

WTIG parameters:

Turbine: S_{B1}=4.5 MW, S_{B2}=3 MW, S_{B3}=1.5 MW, base wind speed =9 m/s, β controller K_p=5, K_i=25, max β =45^0.

Generator:S_{B1}=4.5 MVA, S_{B2}=3 MVA, S_{B3}=1.5 MVA, V=575V, f= 60 Hz, R_s= 0.004843, L_s= 0.1248, R_r'= 0.004377, L_r'=0.1791, L_m=6.7, H=5.04, F=0.01, p=3.

REFERENCES

[1] OECD/IEA, Wind Power Integration into Electricity Systems, Case Study 5, [Online]. Available: http://www.oecd.org/env/cc/

[2] F. Jurado and J. Carpio, "Enhancing the distribution networks stability using distributed generation," *The International Journal for Computation and Mathematics in Electrical and Electronic Engineering*, vol. 24, no. 1, 2005, pp. 107-26.

[3] Vijay Vittal, "Consequence and impact of electric utility industry restructuring on transient stability and small-signal stability analysis," *IEEE Proceedings*, vol. 88, no. 2, 2000, pp. 196-207.

[4] N. D. Hatziargyriou and A. P. S. Meliopoulos, "Distributed energy sources: technical challenges," *IEEE Power Engineering Society Winter Meeting,* vol. 2, 2002, pp. 1017 – 1022.

[5] R. Gnativ and J. V. Milanovi, "Voltage sag propagation in systems with embedded generation and induction motors," IEEE Power Engineering Society Summer Meeting, vol. 1, 2001, pp. 474 – 479.

[6] SimPowerSystems User guide. Available http://www.mathworks.co

Sidhartha Panda received the M.E. degree in Power Systems Engineering from University College of Engineering, Burla, Sambalpur University, India in 2001. Currently, he is a Research Scholar in Electrical Engineering Department of Indian Institute of Technology Roorkee, India. He was an Associate Professor in the Department of Electrical and Electronics Engineering, VITAM College of Engineering, Andhra Pradesh, India and Lecturer in the Department of Electrical Engineering, SMIT, Orissa, India. His areas of research include power system transient stability, power system dynamic stability, FACTS, optimization techniques, distributed generation and wind energy.

Narayana Prasad Padhy was born in India and received his Degree (Electrical Engineering), Masters Degree (Power Systems Engineering) with Distinction and Ph.D., Degree (Power Systems Engineering) in the year 1990, 1993 and 1997 respectively in India. Then he has joined the Department of Electrical Engineering, Indian Institute of Technology (IIT) India, as a Lecturer, Assistant Professor and Associate Professor during 1998, 2001 and 2006 respectively. Presently he is working as a Associate Professor in the Department of Electrical Engineering, Indian Institute of Technology (IIT) India. He has visited the Department of Electronics and Electrical Engineering, University of Bath, UK under BOYSCAST Fellowship during 2005-06 . His area of research interest is mainly Power System Privatization, Restructuring and Deregulation, Transmission and Distribution network charging, Artificial Intelligence Applications to Power System and FACTS.